Development 135, 2637-2648 (2008) doi:10.1242/dev.022244

Temporal requirements of the fragile X mental retardation protein in the regulation of synaptic structure

Cheryl L. Gatto and Kendal Broadie*

Fragile X syndrome (FraX), caused by the loss-of-function of one gene (*FMR1*), is the most common inherited form of both mental retardation and autism spectrum disorders. The *FMR1* product (FMRP) is an mRNA-binding translation regulator that mediates activity-dependent control of synaptic structure and function. To develop any FraX intervention strategy, it is essential to define when and where FMRP loss causes the manifestation of synaptic defects, and whether the reintroduction of FMRP can restore normal synapse properties. In the *Drosophila* FraX model, dFMRP loss causes neuromuscular junction (NMJ) synapse over-elaboration (overgrowth, overbranching, excess synaptic boutons), accumulation of development-arrested satellite boutons, and altered neurotransmission. We used the Gene-Switch method to conditionally drive dFMRP expression to define the spatiotemporal requirements in synaptic mechanisms. Constitutive induction of targeted neuronal dFMRP at wild-type levels rescues all synaptic architectural defects in *Drosophila Fmr1* (*dfmr1*)-null mutants, demonstrating a presynaptic requirement for synapse structuring. By contrast, presynaptic dFMRP expression does not ameliorate functional neurotransmission defects, indicating a postsynaptic dFMRP requirement. Strikingly, targeted early induction of dFMRP effects nearly complete rescue of synaptic structure defects, showing a primarily early-development role. In addition, acute dFMRP expression at maturity partially alleviates *dfmr1*-null defects, although rescue is not as complete as either early or constitutive dFMRP expression, showing a modest capacity for late-stage structural plasticity. We conclude that dFMRP predominantly acts early in synaptogenesis to modulate architecture, but that late dFMRP introduction at maturity can weakly compensate for early absence of dFMRP function.

KEY WORDS: *Drosophila*, Gene-Switch, Neuromuscular junction, Bouton, Futsch

INTRODUCTION

The fragile X syndrome (FraX) mental retardation and autism spectrum disorder, which has a prevalence of ~1:4000 males and 1:6000 females, is among the most common inherited neurological diseases (Koukoui and Chaudhuri, 2007; Penagarikano et al., 2007). Loss of fragile X mental retardation protein (FMRP) expression is the sole cause of the disease state. FMRP is an mRNA-binding protein that regulates mRNA stability and translation for a number of synaptic and cytoskeleton-associated proteins (Castets et al., 2005; Lu et al., 2004; Muddashetty et al., 2007; Reeve et al., 2005; Todd et al., 2003; Zalfa et al., 2007; Zhang et al., 2001). FMRP function regulates the activity-dependent control of synaptic connections via intersection with group 1 metabotropic glutamate receptor (mGluR) signaling (Antar et al., 2004; Bear et al., 2004; Ferrari et al., 2007; Huber et al., 2002; Nosyreva and Huber, 2006; Pan and Broadie, 2007; Pan et al., 2008). The synapsopathic clinical manifestations of the disease include mild to severe mental retardation (Penagarikano et al., 2007), delayed and depressed developmental trajectories (Bailey et al., 2001a; Bailey et al., 2001b), deficits in short-term memory (Cornish et al., 2001; Munir et al., 2000), hyperactivity (Einfeld et al., 1991), disordered sleep (Gould et al., 2000), seizures (Sabaratnam et al., 2001), and the cytological presentation of long, immature-looking cortical dendritic spines, indicating inappropriate development and/or failure of pruning and synapse elimination (Hinton et al., 1991; Rudelli et al., 1985).

Department of Biological Sciences, Kennedy Center for Research on Human Development, Vanderbilt University, Nashville, TN 37232 USA.

*Author for correspondence (e-mail: kendal.broadie@vanderbilt.edu)

Accepted 28 May 2008

Understanding FraX pathogenesis, and subsequently designing effective FraX interventions, requires knowledge of the temporal requirement(s) of FMRP function. A fundamental need is to determine whether FraX is primarily a 'developmental disease', reflecting a transient role for FMRP in progressive neuronal maturation, a 'plasticity disease', reflecting a maintained, constitutive requirement for FMRP at maturity, or some combination of a two-phase requirement giving rise to different FraX symptoms. This study aims to begin resolving this vital question using our well-characterized *Drosophila* FraX disease model (Zhang et al., 2001). *Drosophila Fmr1* (*dfmr1*)-null mutants are fully viable but display impaired learning and memory (Dockendorff et al., 2002), arrhythmic circadian motor activity (Dockendorff et al., 2002; Inoue et al., 2002), over-elaboration of neuronal structure (Michel et al., 2004; Morales et al., 2002; Pan et al., 2004; Zhang et al., 2001), and altered neuronal function (Zhang et al., 2001). The primary synaptic model is the neuromuscular junction (NMJ), which displays increased synapse arborization and branching, increased synaptic bouton number, and elevated neurotransmission. As in mammals, *Drosophila* FMRP (dFMRP) functionally interacts with mGluR-mediated synaptic glutamatergic signaling in the regulation of postsynaptic glutamate receptor expression (Pan and Broadie, 2007) and in sculpting presynaptic architecture (Pan et al., 2008).

In this study, we use the conditional, transgenic Gene-Switch (GS) method (Osterwalder et al., 2001) to drive wild-type dFMRP expression in *dfmr1*-null mutants. This approach allows targeted dFMRP expression during discrete temporal windows, enabling the definition of critical periods of function. We show that constitutive neuronal dFMRP expression rescues all NMJ synaptic structural defects, demonstrating a strictly presynaptic dFMRP requirement, with a mechanistic role in microtubule cytoskeleton regulation. By contrast, targeted presynaptic dFMRP expression does not rescue neurotransmission function in the null mutant, indicating a separable

postsynaptic dFMRP requirement. Temporally, we show that transient early-development expression of dFMRP strongly rescues all facets of synaptic architecture, demonstrating an early role for dFMRP in establishing synapse morphology. We also show that acute dFMRP expression at maturity weakly rescues a subset of synaptic structure defects, showing that dFMRP can mediate some structural plasticity and that late-stage intervention might be beneficial.

MATERIALS AND METHODS

Drosophila genetics

Fly stocks were maintained at 25°C on standard medium. The w^{1118} line served as the genetic background control for the *dfmr1* null. Recombinant parental lines harboring the *dfmr1*-null allele ($dfmr1^{50M}$) (Zhang et al., 2001) and either a wild-type *dfmr1* transgene under UAS control (UAS-9557-3) (Zhang et al., 2001) or the neuronal-specific driver *elav*-Gene-Switch construct (GSG-301) (Osterwalder et al., 2001) were generated using standard genetic techniques. Henceforth, 'GS' as a genotype descriptor refers to the following: $dfmr1^{50M}$, *elav*-GSG-301/$dfmr1^{50M}$, UAS-9557-3. For RU486 (mifepristone; Sigma, St Louis, MO) dosing, the drug was dissolved in 80% ethanol (EtOH) and mixed with food to the desired concentration (shown in figures as GS+RX with RU486 in μg/mL). For vehicle control, the equivalent volume of EtOH was used to identically treat the GS line (GS+E). GS animals were either constitutively raised on supplemented/control food or transferred at staged times as indicated.

Western blot analyses

The central nervous system (CNS), including the brain and the ventral nerve cord (VNC), was dissected free from staged and treated larvae in Ca^{2+}-free modified Jan's standard saline (Jan and Jan, 1976). Dissected CNS samples were homogenized and boiled in 1× NuPage sample buffer (Invitrogen, Carlsbad, CA) supplemented with 40 mM DTT. The total protein from 2-6 brains per sample (depending on larval age) was loaded onto 4-12% Tris-bis acrylamide gels and electrophoresed in NuPage MES buffer (Invitrogen) for 1 hour at 200 V. Transfer to nitrocellulose was carried out for 1 hour at 100 V in NuPage transfer buffer (Invitrogen)/10% methanol. Processing was completed using the Odyssey near-infrared fluorescence detection system (Li-COR, Lincoln, NE) to enable quantitative western blot analysis. Antibodies used included: anti-dFMRP [1:3000; 6A15 (monoclonal), Sigma], anti-α-Tubulin [1:100,000; B512 (monoclonal), Sigma] and Alexa-Fluor 680-conjugated goat anti-mouse (1:10,000; Invitrogen-Molecular Probes). Raw integrated intensities were calculated for dFMRP for the lower molecular weight band of the doublet and for the α-Tubulin band. The ratio of dFMRP:α-Tubulin was used to normalize for loading.

Immunohistochemistry

Staged animals were dissected in standard saline and then fixed for 40 minutes with 4% paraformaldehyde/4% sucrose in PBS (pH 7.4). Preparations were rinsed with PBS, then blocked and permeablized with 0.2% Triton X-100 in PBS (PBST) containing 1% bovine serum albumin (BSA) and 0.5% normal goat serum (NGS) for 1 hour at room temperature. Primary and secondary antibodies were diluted in PBST containing 0.2% BSA and 0.1% NGS and incubated overnight at 4°C and 2 hours at room temperature, respectively. Antibodies used included: anti-dFMRP (1:500; 6A15), anti-Discs large (DLG) [1:200; 4F3 (monoclonal), Developmental Studies Hybridoma Bank (DSHB), University of Iowa], anti-Futsch [1:200; 22C10 (monoclonal), DSHB], anti-horseradish peroxidase (HRP) [1:250; (polyclonal), Sigma], and Alexa-Fluor-conjugated secondaries (1:250; Invitrogen-Molecular Probes). All fluorescent images were collected using a Zeiss LSM 510 META laser-scanning confocal microscope.

Synaptic structure analyses

The muscle 4 NMJ of abdominal segment 3 was used for all quantification. Values were determined for both left and right hemisegments; averaged for each n=1. Synapse junctional area was measured as the maximal cross-sectional area in a maximum projection of each collected z-stack. A synaptic branch was defined as an axonal projection with at least two synaptic boutons. Two bouton classes were defined: (1) type Ib (>2 μm diameter) and (2) mini/satellite (≤2 μm diameter and attached to a type Ib bouton of mature size). Each class is reported as number per terminal. ImageJ (http://rsb.info.nih.gov/ij/) was used for fluorescence intensity thresholding, automated regional outline and area calculation.

FM1-43 assays

Staged animals were dissected in standard saline (containing 0.2 mM $CaCl_2$). NMJ preparations were loaded with FM1-43 (10 μM; Invitrogen-Molecular Probes) using depolarizing 90 mM KCl standard saline (containing 1.8 mM $CaCl_2$) for 5 minutes, washed and imaged. Preparations were then unloaded with the same stimulation for 2 minutes in the absence of FM1-43, washed and imaged. For quantification, only the muscle 4 NMJ in abdominal segments A2-A4 was used. Average fluorescence intensity values and bouton areas were measured from three NMJs per animal, with six individual boutons per NMJ assayed, and then averaged to generate a single data point (n=1 from 18 boutons). The fluorescence intensity units (FIU) measured per bouton are shown, together with the ratio of FM1-43 unload:load fluorescence intensity.

Electrophysiology

Two-electrode voltage-clamp recordings were made at 18°C from muscle 6 in abdominal segments A2-A4 of wandering third instar larvae to examine miniature excitatory junctional currents (mEJCs) (Zhang et al., 2001). Borosilicate glass electrodes were filled with 3 M KCl in standard saline containing: 128 mM NaCl, 2 mM KCl, 4 mM $MgCl_2$, 70 mM sucrose, 5 mM HEPES (pH 7.2) and 0.2 mM $CaCl_2$. Tetrodotoxin (3 μM; Sigma) was added to block action potentials. Each n=1 results from 240 seconds of gap-free recording from independent animals. Traces were filtered using a low-pass 8-pole Bessel filter with –3 dB cut-off of 0.5 kHz. Data were analyzed using Clampfit 9.2 (Molecular Devices, Sunnyvale, CA) using template-based event detection. All traces were analyzed for mean peak amplitude (nA) and frequency (Hz).

Statistics

Statistical analysis was performed using GraphPad InStat 3 (GraphPad Software, San Diego, CA). Generally, unpaired t-tests were used to compare means of control and *dfmr1*-null, and Tukey-Kramer multiple comparisons tests were applied to all GS categories. In FM1-43 experiments, Dunnet's multiple comparison tests were also used to compare each value independently with the stated control. Significance levels in figures are represented as $P<0.05$ (*); $P<0.01$ (**); $P<0.001$ (***). Error bars represent s.e.m.

RESULTS

Targeted conditional expression of *Drosophila* FMRP in the nervous system

The conditional Gene-Switch (GS) method utilizes a modified UAS-GAL4 system that provides a means of tightly regulating tissue-specific transgene expression in order to define spatiotemporal requirements (McGuire et al., 2004; Osterwalder et al., 2001). GS-GAL4 lines are dependent on the progesterone analog RU486 (mifepristone) to drive hormone-responsive UAS-construct expression (Fig. 1A). We have driven a UAS-*dfmr1* transgene with neuronal *elav*-GS GAL4 in the *dfmr1*-null mutant background to determine spatial and temporal requirements for dFMRP at the NMJ synapse. Thus, we assayed, in a targeted fashion, the presynaptic roles of dFMRP in synapse assembly and function following constitutive expression and timed intervention windows.

The critical first step was to determine RU486 dosage sufficient to match dFMRP levels in the wild type, so that the transgenic protein is not under- or overexpressed. RU486 dosage-dependence tests were conducted by assaying dFMRP expression in the larval CNS by western blot (Fig. 1B,C) and by in situ immunohistochemistry (Fig. 1D). Analyses were performed on wild-type control (w^{1118}), *dfmr1*-null and *dfmr1*-null animals harboring both the *elav*-GS GAL4 driver and UAS-*dfmr1* transgene

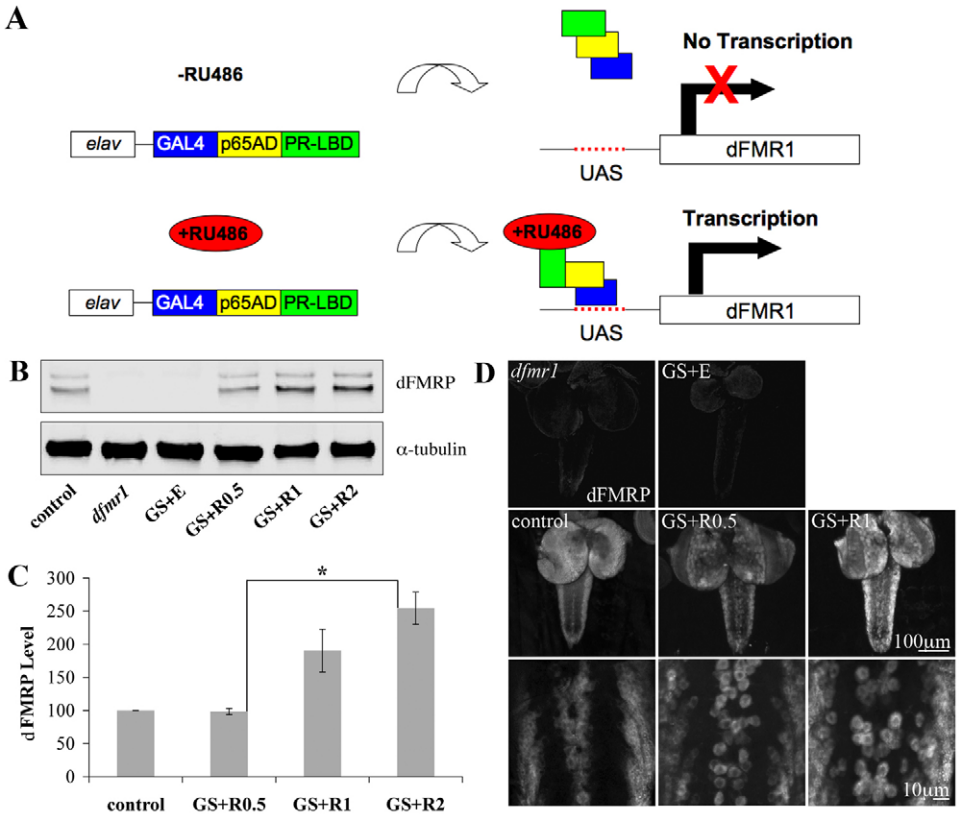

Fig. 1. Gene-Switch system drives targeted dFMRP expression in neurons. (**A**) Schematic of the Gene-Switch (GS) system. The GAL4 DNA-binding domain is fused to the p65 activation domain (p65AD) and a mutated progesterone receptor ligand-binding domain (PR-LBD). In the absence of RU486, the GS is 'off'. In the presence of RU486, the hormone-responsive GAL4 drives dFMRP transcription downstream of the UAS regulatory sequence. This approach allows spatial and temporal control of dFMRP expression in the *dfmr1*-null background. (**B**) Western blot of isolated third instar *Drosophila* larval CNS. Genotypes as indicated: w^{1118} (control), homozygous $dfmr1^{50M}$ null allele (*dfmr1*) and $dfmr1^{50M}$, *elav*-GSG-301/$dfmr1^{50M}$, UAS-9557-3 (GS). Treatment as indicated: GS fed ethanol vehicle (GS+E) or RU486 (GS+RX, where X is the RU486 concentration in μg/mL). Blot was probed for dFMRP and α-Tubulin, illustrating RU486 dosage responsiveness. (**C**) Quantification of western blot dFMRP levels. Individual band intensities were normalized to α-Tubulin and expressed as a percentage of the control. Bars indicate mean±s.e.m. **P*<0.05. (**D**) dFMRP immunohistochemistry of wandering third instar larvae CNS. Bottom row of panels shows higher magnification views of dFMRP staining in the VNC. Note the RU486 dosage dependence of dFMRP expression.

(henceforth referred to as GS animals), constitutively fed with RU486 (GS+R) or with ethanol vehicle only (GS+E). Feeding with 0.5 μg/mL RU486 yielded dFMRP levels closely approximating that of the wild-type control (98±5%), whereas 1 and 2 μg/mL RU486 induced progressive overexpression (190±32% and 255±25% compared with control, respectively; 2 μg/mL versus control, $P<0.05$; Fig. 1C). Thus, in GS animals, RU486 drives dose-dependent expression of dFMRP in the nervous system, and a dosage of 0.5 μg/mL fed constitutively generates dFMRP expression indistinguishable from those of the wild type.

Presynaptic dFMRP expression rescues *dfmr1*-null synapse architecture

In the *Drosophila* FraX model, loss of dFMRP causes NMJ over-elaboration (including excessive branching, overgrowth and supernumerary synaptic boutons), accumulation of mini- or satellite boutons, and altered functional neurotransmission properties due to both pre- and postsynaptic defects (Zhang et al., 2001). To quantify branching, individual projections harboring more than two boutons were counted as synaptic branches (control 3.0±0.3 branches versus *dfmr1*-null 4.8±0.2 branches, $n=12$, $P<0.001$; Fig. 2A,B). To quantify synaptic area, the junction was delimited by either HRP (presynaptic) or DLG (postsynaptic) and the area measured (for example, HRP – control 160±8 μm^2 versus *dfmr1*-null 241±12 μm^2, $n=12$, $P<0.001$; Fig. 2C,D). Lastly, type Ib bouton numbers per terminal were counted, partitioned into either mature boutons (control 19±1 boutons versus *dfmr1*-null 29±1 boutons, $n=12$, $P<0.001$; Fig. 2F) or mini/satellite boutons based on size and relative positioning (control 0.6±0.2 mini-boutons versus *dfmr1*-null 3.7±0.4 mini-boutons, $n=12$, $P<0.001$; Fig. 2E,G).

We tested for rescue of architectural defects upon constitutive presynaptic dFMRP induction. NMJs were double-labeled with anti-HRP, to delineate the innervating presynaptic neuron, and with anti-DLG, to reveal the postsynaptic domain of the target muscle (Fig. 2A). GS animals fed with vehicle (EtOH) fully phenocopied the *dfmr1*-null with respect to all structural abnormalities (Fig. 2). By sharp contrast, constitutively RU486-fed animals were completely rescued, with entirely normal synaptic architecture. Presynaptically targeted dFMRP was assayed with two RU486 dosages: 0.5 μg/mL (wild-type dFMRP level; Fig. 1C) and 2.0 μg/mL (significantly elevated dFMRP; Fig. 1C). As predicted, the wild-type-control-matched dFMRP expression provided the most exact rescue of synaptic structure features. First, synaptic branch number was perfectly rescued from the elevated branching that characterizes the

null mutant [GS+E 4.5±0.3 branches versus GS+RU486 (0.5 μg/mL) 3.0±0.3 branches, n=12, P<0.001; Fig. 2B]. Second, both pre- and postsynaptic areas were restored to control levels [for example, HRP junctional area – GS+E 255±16 μm^2 versus GS+RU486 (0.5 μg/mL) 150±7 μm^2, n=12, P<0.001; Fig. 2C,D]. Finally, the overproliferation of synaptic boutons was rescued for both the large, mature boutons [GS+E 28±1 boutons versus GS+RU486 (0.5 μg/mL) 17±1 boutons, n=12, P<0.001; Fig. 2F] and the small, immature satellite boutons [GS+E 3.4±0.3 mini-boutons versus GS+RU486 (0.5 μg/mL) 0.3±0.1 mini-boutons, n=12, P<0.001; Fig. 2G]. These findings demonstrate an entirely presynaptic requirement for dFMRP in synaptic structuring.

Temporal control of dFMRP expression in the nervous system

Having confirmed GS system utility for examining morphological rescue strategies, we next moved to presynaptic dFMRP induction during discrete temporal windows. To test developmental roles in the establishment of synaptic organization, early GS induction of dFMRP was first examined. GS animals were treated with RU486 within 3 hours of hatching for a brief period of 12 hours (Fig. 3A). Neuronal dFMRP levels were then immediately analyzed for comparison to that of the wild-type control (Fig. 3B). RU486 fed at 0.1 μg/mL yielded dFMRP levels closest to that of the control at 142±48%, whereas higher concentrations of RU486 induced steep, dosage-dependent overexpression of dFMRP (0.25 and 0.5 μg/mL induced 397±128% and 556±268%, respectively; Fig. 3C).

The duration of dFMRP expression was analyzed by monitoring dFMRP levels at timed periods following withdrawal of RU486 (Fig. 3D). At 24 hours post-treatment, there was a ~70% reduction relative to the initial, induced dFMRP level, irrespective of RU486 dosage (0.1 μg/mL RU486 45±23%, and 0.25 μg/mL RU486 107±17%, as compared with control; Fig. 3E). Loss of dFMRP was progressive, with levels after 0.1 μg/mL RU486 treatment declining to 35±8% at 48 hours, 10±2% at 60 hours and undetectable by 72 hours post-treatment (Fig. 3E). These studies indicate that dFMRP can be rapidly and strongly induced within hours, but that the inherent stability of dFMRP causes persistence during a period of

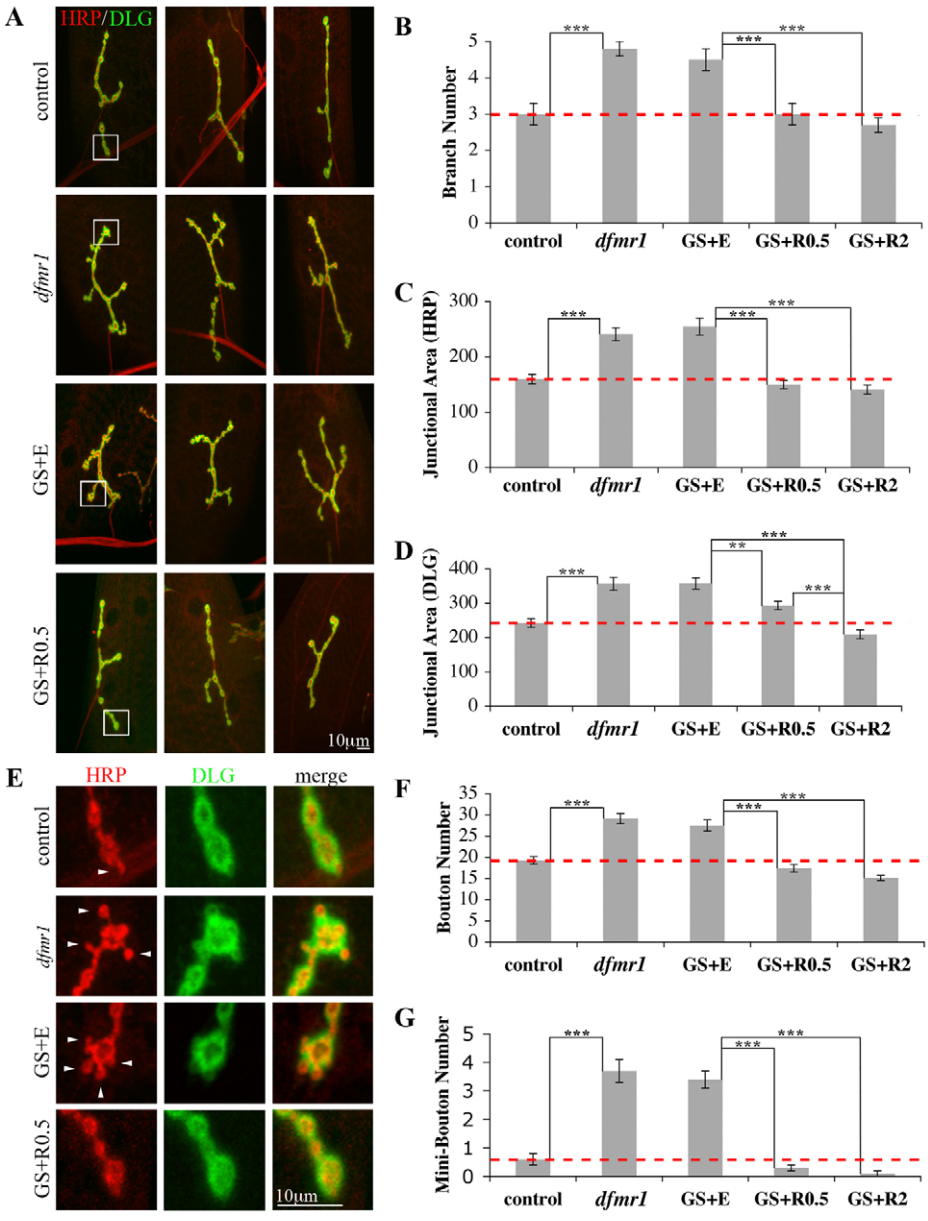

Fig. 2. Targeted presynaptic dFMRP rescues all *dfmr1*-null NMJ structure defects. (**A**) Representative images of wandering third instar *Drosophila* larval NMJs; genotypes and treatments as shown. NMJs co-labeled for HRP (presynaptic marker) and DLG (postsynaptic marker), with three examples of each condition shown. (**B-D**) Quantification of NMJ synaptic branch number and area, defined for presynaptic area (HRP domain) and postsynaptic area (DLG domain). *dfmr1*-null terminals display overgrowth and over-elaboration. GS+E phenocopies *dfmr1*, and complete rescue occurs with RU486 constitutively driving presynaptic dFMRP expression. (**E**) Representative images of mini/satellite boutons; genotypes and treatments as shown. High-magnification images of boxed regions in A showing mini-boutons (arrowheads) in both *dfmr1*-null and GS+E genotypes and their absence following RU486 induction. (**F**,**G**) Quantification of normal (>2 μm diameter) and mini-bouton (≤2 μm diameter, attached to a normal bouton) number per NMJ in genotypes and treatments shown. n=12 animals for all conditions. Bars indicate mean±s.e.m. Dashed red lines highlight control level quantifications. **P<0.01, ***P<0.001.

gradual decline. Analysis of normalized dFMRP:α-Tubulin intensity values indicates an apparent dFMRP half-life of 25.5±1.7 hours. This measured relative stability of dFMRP therefore limits the resolution of temporal expression windows.

Early dFMRP induction fully rescues *dfmr1*-null synaptic structure defects

Both FraX patients and *Fmr1*-knockout (KO) mice display an increased number of immature-appearing synaptic spines, similar to those occurring during neocortical development (Comery et al., 1997; Galvez and Greenough, 2005; Hinton et al., 1991; Irwin et al., 2001; Nimchinsky et al., 2001; Rudelli et al., 1985). In *Fmr1* mutant mice, these aberrant synapses are developmentally transient and disappear, but then reappear later in the mature animal (Galvez and Greenough, 2005; Nimchinsky et al., 2001). These developmental dynamics suggest specific functions for FMRP during defined windows, especially early in synaptogenesis. To test this hypothesis in our model, dFMRP expression was induced for a brief 12-hour window immediately following hatching (Fig. 3A) and mature third instar larvae were collected 72 hours post-treatment [~108 hours after egg lay (AEL)], with NMJ synapses co-labeled for HRP and DLG to compare RU486-treated with the EtOH-treated control (Fig. 4A). RU486 concentrations of 0.1 μg/mL and 0.25 μg/mL were analyzed, representing normal and overexpression levels, respectively.

Significant and complete rescue of the *dfmr1*-null structural phenotypes was observed with transient early expression of dFMRP (Fig. 4B-E). The synaptic overbranching that is characteristic of the *dfmr1*-null was fully rescued at the higher dFMRP level [GS+E 4.8±0.2 branches, n=14, versus GS+RU486 (0.25 μg/mL) 3.4±0.1 branches, n=12, P<0.001; Fig. 4B]. The greater synaptic bouton number was similarly restored to the wild-type level (GS+E 27±1 boutons, n=14, versus both 0.1 μg/mL and 0.25 μg/mL GS+RU486 21±1 boutons, n=12, P<0.01; Fig. 4C). Finally, the increased synaptic junction area was rescued by both dFMRP levels; for example, the HRP presynaptic area was comparable under both conditions [GS+E 206±8 μm^2, n=14, versus both GS+RU486 (0.1 μg/mL) 163±8 μm^2, n=12, P<0.01, and GS+RU486 (0.25 μg/mL) 178±7 μm^2, n=12, P<0.05; Fig. 4D,E]. These findings indicate a specific early developmental requirement for dFMRP in sculpting synaptic architecture. Further, the persistence of normal synaptic structure at the mature NMJ in the absence of dFMRP suggests that it is not required for the maintenance or stability of synaptic structure once established.

Late intervention partially restores *dfmr1*-null synaptic structure defects

A crucial question for FraX patients is whether late correction of the FMRP deficit can ameliorate disease symptoms. Having identified the early role for dFMRP in the establishment of NMJ synaptic morphology, we next examined whether reintroduction of dFMRP into mature animals could rescue synapse structural defects. GS animals were treated with either RU486 or EtOH for 12 hours at a mature larval time point (96-108 hours AEL; Fig. 5A) and then immediately analyzed. Protein level comparisons showed that RU486 fed at 1-2 μg/mL drives dFMRP levels that are indistinguishable from that of the wild-type control (99±9% and 90±6%, respectively), whereas RU486 at 5 μg/mL elevates dFMRP to 227±21% of control (compared with both 1 and 2 μg/mL, P<0.01

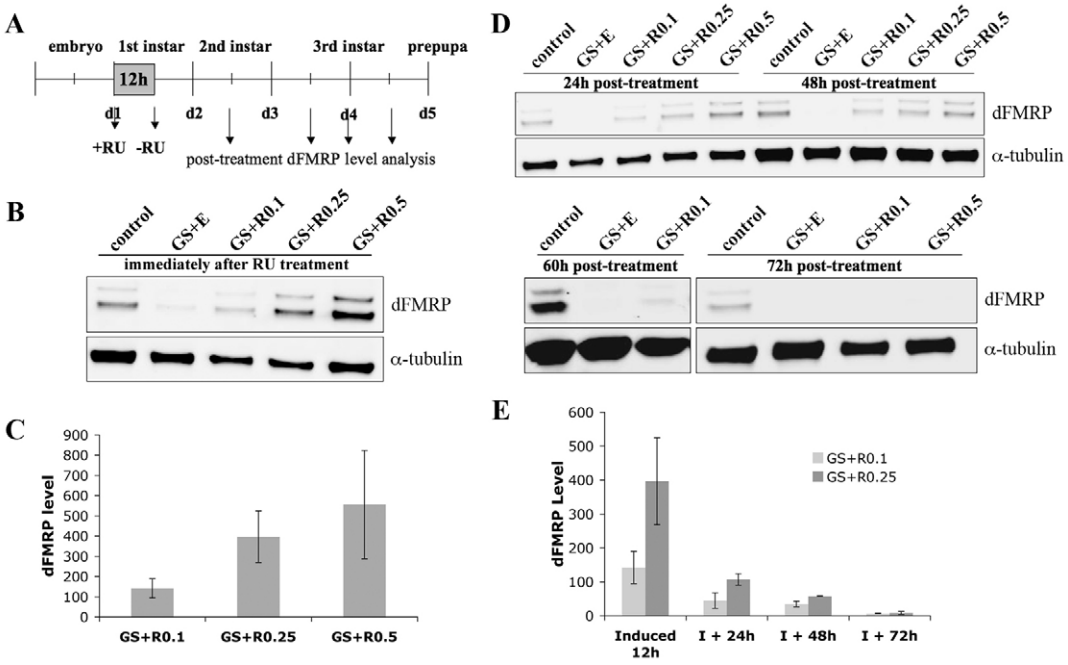

Fig. 3. Temporal control of dFMRP expression by acute early RU486 treatment. (**A**) Depiction of time line employed for early *Drosophila* larval induction of dFMRP indicating points of dFMRP protein analyses. (**B**) Representative western blot of first instar larval CNS probed for dFMRP and α-Tubulin. Samples were taken immediately after a 12-hour treatment with RU486 as indicated. (**C**) Quantification of western blot dFMRP levels. Individual band intensities were normalized to α-Tubulin and expressed as a percentage of the control. Bars indicate mean±s.e.m. (**D**) Representative western blots of second and third instar larval CNS. dFMRP levels progressively diminish and are minimally detectable 60 hours post-treatment. (**E**) Quantification of dFMRP levels as a function of age. Individual band intensities were normalized to α-Tubulin and expressed as a percentage of the control. Bars indicate mean±s.e.m.

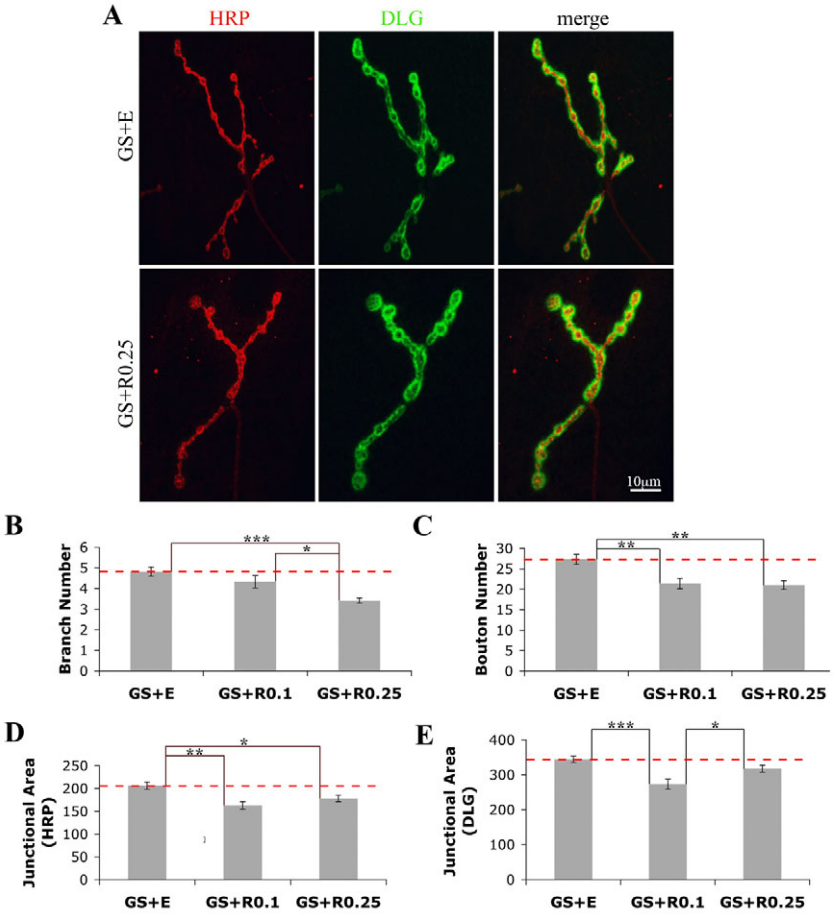

Fig. 4. Early presynaptic dFMRP rescues *dfmr1*-null NMJ architectural phenotypes.
(**A**) Representative images showing NMJs from *Drosophila* either vehicle- (GS+E) or experimentally treated (GS+RU486 at 0.25 mg/mL, R0.25) for 12 hours immediately post-hatching and then analyzed as third instar larvae (108 hours AEL), co-labeled for HRP and DLG. (**B-E**) Quantification of NMJ structure. Statistically significant rescue occurs for synaptic branch number (B), synaptic bouton number (C), presynaptic junctional area (D), and postsynaptic junction area (E). *n*=12-14 animals for each condition. Bars indicate mean±s.e.m. Dashed red lines highlight *dfmr1*-null conditions. **P*<0.05, ***P*<0.01, ****P*<0.001.

and *P*<0.001, respectively; Fig. 5B,C). Both the low (1 μg/mL) and high (5 μg/mL) RU486 induction levels were used to examine the effect on synaptic architecture.

Examination of NMJ structure following late intervention showed slight but significant rescue of a subset of defects (Fig. 5D). There was no rescue of either branching or synapse area (data not shown). However, the increased synaptic bouton number (GS+E 27±1 boutons, *n*=12) was significantly reduced following the 12-hour acute intervention [GS+RU486 (1 μg/mL) 22±1 boutons, *n*=12, and GS+RU486 (5 μg/mL) 23±1 boutons, *n*=11, *P*<0.01; Fig. 5E]. Thus, late intervention using the GS system to induce targeted presynaptic dFMRP mediates a weak, partial rescue of synaptic structural phenotypes. This finding indicates both maintained morphological plasticity at the NMJ synapse and at least modest reversal potential for specific mutant phenotypes.

Presynaptic dFMRP expression rescues *dfmr1*-null synaptic cytoskeleton defects

In addition to synaptic architecture, we examined the synaptic organization of the known dFMRP target Futsch, the microtubule-associated MAP1B homolog (Hummel et al., 2000). Futsch is negatively regulated by dFMRP, and *dfmr1; futsch* double-mutants display normal NMJ architecture (Zhang et al., 2001). Futsch is required for dendritic, axonal and synaptic development (Bettencourt da Cruz et al., 2005; Roos et al., 2000; Ruiz-Canada et al., 2004). In wandering third instar larvae, *dfmr1*-null synapses were found to contain significantly elevated numbers of Futsch-positive cytoskeletal loops within synaptic boutons (control 2.0±0.4 loops, *n*=11, versus *dfmr1*-null 4.3±0.4 loops, *n*=12, *P*<0.001; Fig. 6A,B). In control animals, the loop structures were usually restricted to terminal boutons. By contrast, *dfmr1*-null NMJs displayed Futsch-positive loop structures abnormally interspersed throughout the entire synaptic arbor (Fig. 6A). GS vehicle-fed animals phenocopied the *dfmr1*-null, and the defect was partially rescued by constitutively expressing dFMRP [GS+E 4.7±0.2 loops, *n*=12, versus both GS+RU486 (0.5 μg/mL) 3.5±0.4 loops, *n*=12, *P*<0.05, and GS+RU486 (2 μg/mL) 3.2±0.3 loops, *n*=13, *P*<0.01; Fig. 6B].

Examining temporal windows of GS intervention, we observed that 12-hour RU486 treatment at either early or mature larval time points restored a more normal cytoskeletal arrangement when examined at 108 hours AEL. In the early treatment window, complete rescue was observed only at the higher RU486 dosage [GS+E 7.8±0.4 loops, *n*=11, versus GS+RU486 (0.25 μg/mL) 5.2±0.3 loops, *n*=12, *P*<0.001; Fig. 6C]. In the late treatment, progressive rescue was achieved in a dose-dependent manner with both RU486 concentrations tested [GS+E 8.8±0.6 loops, *n*=15, versus GS+RU486 (1 μg/mL) 6.1±0.2 loops, *n*=10, *P*<0.01, and GS+RU486 (5 μg/mL) 5.8±0.4 loops, *n*=11, *P*<0.001; Fig. 6C]. These findings suggest that the synaptic organization of the Futsch-positive microtubule cytoskeleton remains plastic throughout development and at maturity, and that dFMRP has a constitutively significant role in modulating this mechanism.

Presynaptic dFMRP expression does not rescue *dfmr1*-null synapse function

We next examined the potential for dFMRP induction to rescue synapse functional properties. *dfmr1*-null NMJ synapses exhibit a ~2-fold increase in neurotransmission strength (Zhang et al., 2001),

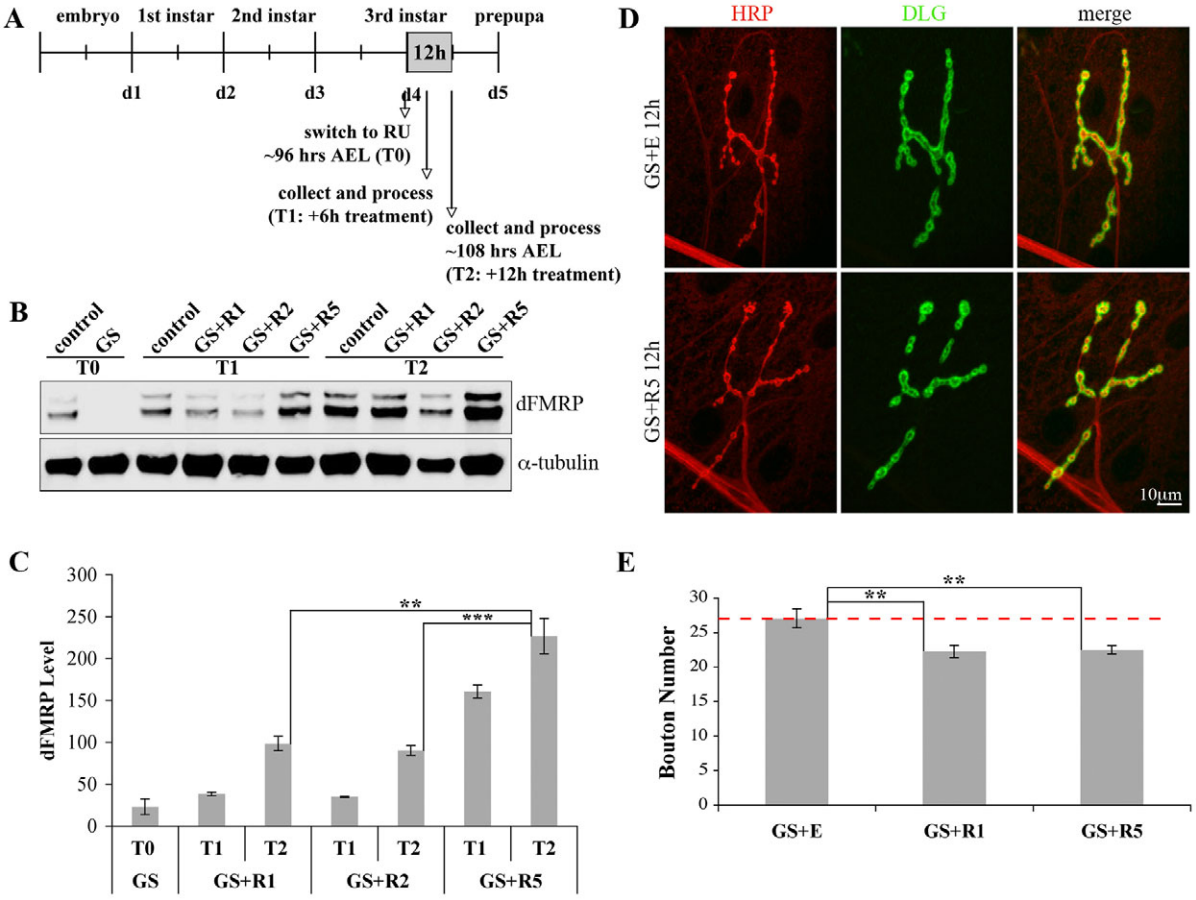

Fig. 5. Acute late presynaptic dFMRP partially rescues *dfmr1*-null NMJ structure. (**A**) Depiction of time line employed for late larval stage intervention. *Drosophila* larvae were raised to 96 hours AEL, transferred to RU486-containing food for 12 hours, and then immediately processed. (**B**) Representative western blot of third instar larval CNS probed for dFMRP and α-Tubulin. (**C**) Quantification of western blot dFMRP levels. Individual band intensities were normalized to α-Tubulin and expressed as a percentage of the control. Bars indicate mean±s.e.m. ***P*<0.01, ****P*<0.001. (**D**) Representative NMJ images from animals treated during the late 12-hour time period, co-labeled for HRP and DLG. Acute dFMRP expression reduces the excess number of boutons observed in the *dfmr1*-null. (**E**) Quantification of synaptic bouton number. Late 12-hour treatment with RU486 to induce dFMRP effects partial rescue of NMJ structural alterations. *n*=10-12 animals for each condition. Bars indicate mean±s.e.m. Dashed red line highlights the *dfmr1*-null condition. ***P*<0.01.

but it has not been shown whether the change is due to elevated glutamate release or increased glutamate receptor function. To make this distinction, we used the lipophilic styryl dye FM1-43, which incorporates into the presynaptic vesicle pool, so that its loss or retention can be visualized to monitor activity-dependent vesicle cycling (Brumback et al., 2004; Fergestad and Broadie, 2001; Rohrbough et al., 2004). After a round of stimulated dye loading and unloading (Fig. 7A), a significantly greater amount of the dye was released from mutant than control vesicles (control 0.46±0.04 unload:load, *n*=8, versus *dfmr1*-null 0.31±0.04 unload:load, *n*=8, *P*<0.01; Fig. 7B). The average area assayed per bouton was equivalent (control 9.3±1.5 μm^2, *n*=5, versus *dfmr1*-null 9.2±1 μm^2, *n*=5), ensuring that the differences observed were due to dye cycling rates and not sampling variability. The average fluorescence intensity unit (FIU) values obtained after loading were comparable (control 153±6 FIU versus *dfmr1*-null 153±5 FIU, *n*=5; Fig. 7C), but unloading was more rapid in the mutant (control 81±7 FIU versus *dfmr1*-null 43±4 FIU, *n*=5, *P*<0.01; Fig. 7C). Thus, the depressed level of retained dye in *dfmr1* mutants indicates an enhanced rate of vesicle exocytosis and provides a mechanistic explanation for the elevated evoked synaptic transmission (Zhang et al., 2001).

Surprisingly, constitutive presynaptic dFMRP expression provided no rescue of the FM1-43 functional transmission defect in GS animals [GS+E 0.29±0.02 unload:load, *n*=13; GS+RU486 (0.5 μg/mL) 0.30±0.03 unload:load, *n*=6; GS+RU486 (2 μg/mL) 0.29±0.01 unload:load, *n*=9; Fig. 7B]. Again, actual fluorescence intensity values illustrate the heightened unloading phase and the lack of any phenotypic rescue upon GS induction [load: GS+E 124±8, GS+RU486 (0.5 μg/mL) 130±12, GS+RU486 (2 μg/mL) 127±5, *n*=5; unload: GS+E 33±4, GS+RU486 (0.5 μg/mL) 31±2, GS+RU486 (2 μg/mL) 36±3, *n*=5; Fig. 7C]. Of note, GS animals under all conditions appeared to load at slightly lower absolute levels; however, only the difference seen between w^{1118} control (153±6) and GS+E (124±8) is statistically significant (*P*<0.05). These findings indicate an apparent postsynaptic requirement for dFMRP, with retrograde signaling control of presynaptic function. They also indicate that dFMRP displays differential spatial requirements in relation to synaptic structure and function.

To further examine functional requirements, two-electrode voltage-clamp (TEVC) recordings were made to monitor miniature excitatory junctional currents (mEJCs), as a direct measure of glutamate release (Fig. 8A). The mEJC amplitude was comparable

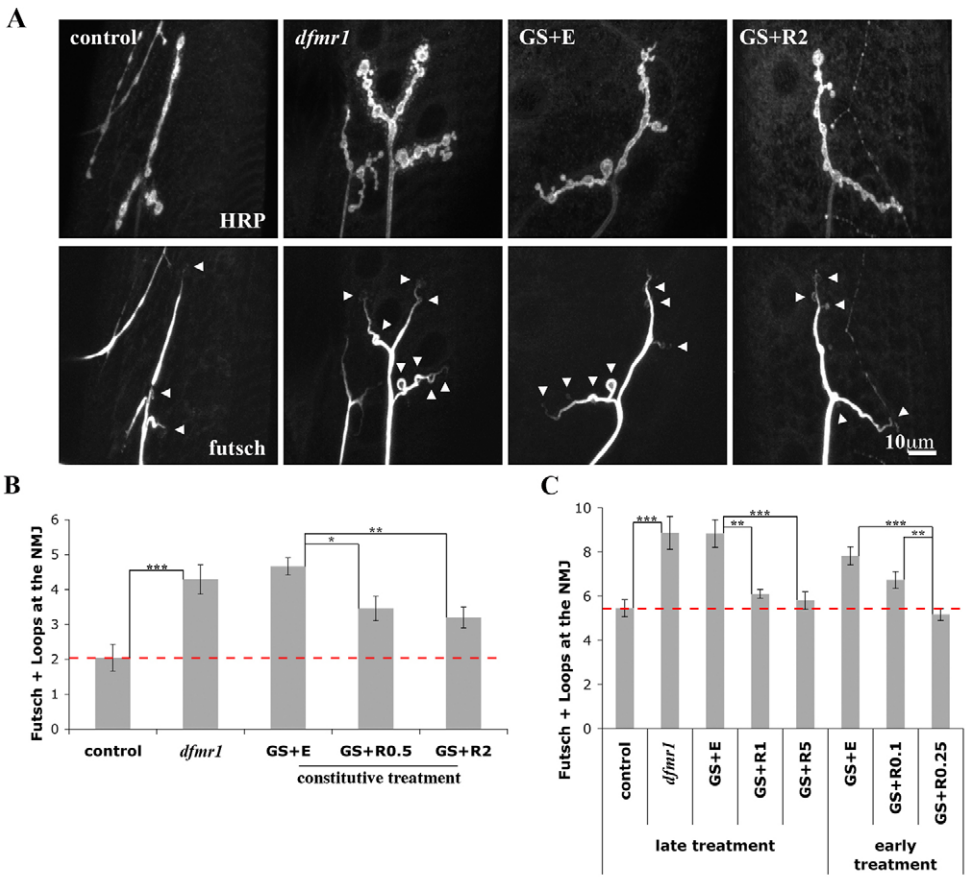

Fig. 6. Targeted presynaptic dFMRP rescues *dfmr1*-null NMJ cytoskeletal defects.
(**A**) Representative images of NMJs from wandering third instar *Drosophila* larvae probed for HRP and Futsch. GS animals were constitutively fed either EtOH vehicle or RU486 at 2 μg/mL. Note the increased number of Futsch loops present throughout the *dfmr1*-null synaptic terminals.
(**B**) Quantification of Futsch loops. In wandering third instar larvae, constitutive treatment with RU486 partially rescues the cytoskeletal alteration of the null mutant. *n*=11-13 animals for each condition.
(**C**) Quantification of Futsch loops after either early or late 12-hour treatment with RU486 (taken at 108 hours AEL). Age-matched control and *dfmr1*-nulls are presented. *n*=10-15 animals for each condition. Bars indicate mean±s.e.m. Dashed red line highlights control level quantifications. **P*<0.05, ***P*<0.01, ****P*<0.001.

between all genotypes, with a modest difference between control (1.01±0.04 nA, *n*=10) and *dfmr1*-null (0.84±0.04 nA, *n*=10, *P*<0.05; Fig. 8B). By contrast, substantial differences were observed in mEJC frequency, with a nearly 3-fold increase in the *dfmr1*-null compared with control (control 1.2±0.2 Hz versus *dfmr1*-null 3.4±0.5 Hz, *n*=10, *P*<0.01; Fig. 8C). Elevated mEJC frequencies were also present in the GS animals (GS+E 2.6±0.2 Hz, *n*=10) and, upon presynaptic dFMRP induction, the condition was markedly exacerbated, not rescued toward control [GS+RU486 (0.5 μg/mL) 5.0±0.7 Hz; GS+RU486 (2 μg/mL) 6.4±0.9 Hz, *n*=10; Fig. 8C]. These findings provide strong support for a postsynaptic dFMRP requirement in regulating synapse function.

DISCUSSION

FraX is caused by the loss of FMRP; however, the spatial and temporal requirements for FMRP are largely unknown. The definition of these requirements in nervous system connectivity, transmission and plasticity is essential for understanding FraX pathophysiology and informing the design of effective FraX therapeutic intervention strategies. In this study, we tackle these questions using the established *Drosophila* FraX model, focusing on the NMJ model synapse. We use the inducible GS system to control spatial and temporal dFMRP expression in an otherwise null mutant. We show that constitutively expressed presynaptic dFMRP fully rescues synapse architecture and cytoskeleton patterning, but does not restore normal synaptic function. We therefore conclude that dFMRP has crucial presynaptic roles controlling synaptic morphology; however, the regulation of neurotransmission strength is mediated by postsynaptic function. We demonstrate that a brief dFMRP pulse early in development is sufficient to meet presynaptic needs controlling synapse configuration, but that a brief pulse at maturity also partially restores normal synapse structure. We therefore conclude that dFMRP plays a primary role early in synapse assembly, but the synapse maintains morphological plasticity. Moreover, late dFMRP reintroduction has some ability to counteract the effects of dFMRP loss throughout development. These conclusions suggest that FraX interventions should be targeted to young children in order to maximize efficacy, but also that restoration, or perhaps circumvention, of FMRP function at maturity could also be beneficial as a FraX treatment strategy.

Spatial requirements for FMRP: presynaptic versus postsynaptic function

Although neurological consequences are readily identifiable in the FraX disease state, the causative spatial defects associated with FMRP loss are largely undefined. The most-studied structural anomaly in FraX patients and *Fmr1* KO mice is increased density of morphologically immature dendritic spines (Comery et al., 1997; Galvez and Greenough, 2005; Hinton et al., 1991; Irwin et al., 2001; Nimchinsky et al., 2001; Rudelli et al., 1985). Although this is commonly treated as a solely postsynaptic defect, spines are synaptic contacts, by definition, so there should be an equivalent defect in opposing presynaptic boutons. Thus, the FMRP requirement could be presynaptic, postsynaptic or both. *Drosophila Fmr1* mutants similarly display synaptic architecture defects in several classes of neurons, including motoneurons (Zhang et al., 2001), lateral and dorsal cluster neurons (Morales et al., 2002), and mushroom body Kenyon cells, a site of learning and memory consolidation (Michel et al., 2004; Pan et al., 2004). At the NMJ,

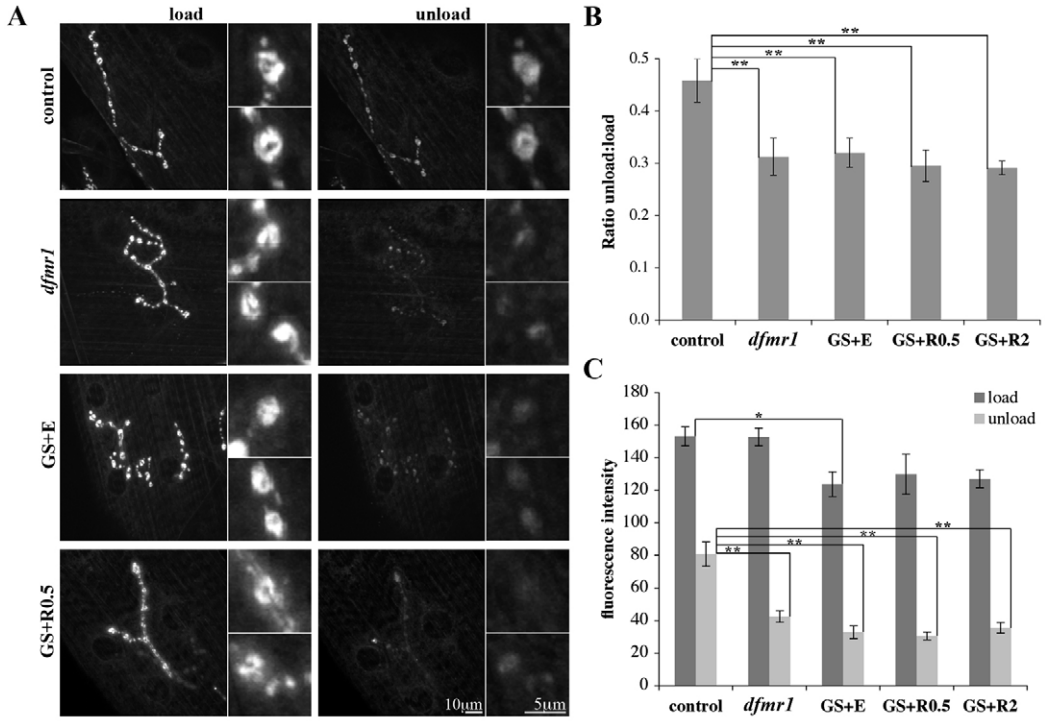

Fig. 7. Constitutive presynaptic dFMRP does not rescue *dfmr1*-null FM1-43 function defect. (**A**) Representative images of wandering third instar *Drosophila* larval NMJs loaded with FM1-43 and then subsequently unloaded with high [K^+] depolarizing saline. Note the elevated relative fluorescence retained in control versus *dfmr1*-null and GS mutants. Insets show representative synaptic boutons at higher magnification. (**B**) Quantification of the FM1-43 unload:load fluorescence intensity ratio. Sample sizes: *n*=8 each control and *dfmr1*-null; *n*=13 GS+E; *n*=6 GS+R0.5; and *n*=9 GS+R2. (**C**) Quantification of average fluorescence intensity per bouton in loaded and unloaded conditions. Sample sizes: *n*=5 for each control, *dfmr1*-null, GS+E, GS+R0.5 and GS+R2. Bars indicate mean±s.e.m. **P*<0.05, ***P*<0.01.

synaptic defects have been attributed to both pre- and postsynaptic roles of dFMRP, as both neuronal and muscle overexpression result in altered architecture (Zhang et al., 2001).

Functionally, the *Fmr1* KO mouse displays decreased cortical long-term potentiation (LTP) (Larson et al., 2005; Li et al., 2002) and increased hippocampal long-term depression (LTD) (Huber et al., 2002; Nosyreva and Huber, 2006). The LTD alteration is suggested to be postsynaptically mediated because FMRP normally functions to suppress translation of dendritic mRNAs to attenuate LTD (Bear et al., 2004); however, no spatial dissection of this function has been reported. In *Drosophila*, loss of dFMRP results in altered neurotransmission in both visual system synapses and at the NMJ (Zhang et al., 2001). In the most-studied NMJ location, elevated neurotransmission has been suggested to be primarily due to a presynaptic role for dFMRP, as neuronal overexpression results in dramatic elevation in spontaneous vesicle fusion events (Zhang et al., 2001). However, variability in functional outputs might reflect differential FMRP roles in trans-synaptic signaling, and decreased

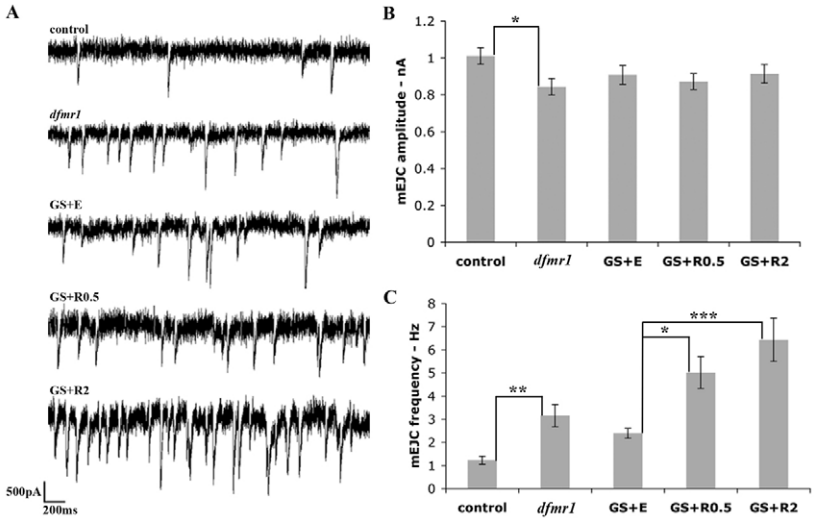

Fig. 8. Constitutive presynaptic dFMRP does not rescue *dfmr1*-null mEJC function defect. (**A**) Sample miniature excitatory junctional current (mEJC) traces from wandering third instar *Drosophila* larval NMJs showing 3 seconds of recording from control, *dfmr1*-null, GS+E, GS+R0.5 and GS+R2. Note the increased number of events in the *dfmr1*-null compared with the control, and the further increase upon dFMRP induction. (**B**) Quantification of mEJC peak amplitude. (**C**) Quantification of mEJC frequency. Bars indicate mean±s.e.m.; *n*=10 for each category. **P*<0.05, ***P*<0.01, ****P*<0.001.

postsynaptic sensitivity is often offset by a compensatory increase in presynaptic release (Davis et al., 1998; Frank et al., 2006; Paradis et al., 2001; Petersen et al., 1997; Plomp et al., 1992; Sandrock et al., 1997).

The current study clearly demonstrates a presynaptic role for dFMRP in regulating NMJ synaptic architecture, including terminal area, synaptic branching, and the formation of synaptic boutons, all of which are negatively regulated by dFMRP function in the presynaptic cell. Perhaps most interesting is the accumulation of mini/satellite boutons in the absence of presynaptic dFMRP function. Work by us and others has suggested that these tiny boutons represent a developmentally arrested state at an otherwise normal stage of bouton maturation (Ashley et al., 2005; Beumer et al., 1999; Dickman et al., 2006; Torroja et al., 1999). Since the *dfmr1*-null also shows a supernumerary abundance of mature synaptic boutons, the accumulation of mini-boutons suggests that the absence of presynaptic dFMRP function triggers the initiation of a disproportionate number of bouton formation events, but that other proteins required for bouton maturation are limiting. Therefore, dFMRP has a primary role in restricting bouton deposition. An early-development pulse of dFMRP prevents the aberrant accumulation of mature boutons, but does not prevent accumulation of mini-boutons. Thus, dFMRP is constitutively required in the presynaptic cell to arrest this nascent stage of synaptic bouton formation.

We established previously that dFMRP acts as a translational repressor of the MAP1B homolog Futsch (Zhang et al., 2001). *dfmr1*-null phenotypes are mimicked by presynaptic overexpression of Futsch, and genetic control of Futsch overexpression in the *dfmr1*-null background completely rescues NMJ overgrowth phenotypes. Subsequent mouse studies revealed the same MAP1B upregulation and associated enhanced microtubule stability in *Fmr1* KO neurons (Lu et al., 2004). At the *Drosophila* NMJ, Futsch binds microtubule hairpin loops in a dynamic subset of synaptic boutons (Roos et al., 2000). In other systems, the appearance of these microtubule structures is linked to the stalling of axonal growth cones (Dent and Kalil, 2001; Tanaka and Kirschner, 1991; Tsui et al., 1984), which predicts a similar role in synapse growth (Roos et al., 2000). In *dfmr1*-nulls, however, there is an increased number of Futsch loops throughout the overgrown NMJ synaptic arbor, a defect rescued by targeted presynaptic dFMRP expression. Furthermore, developmental analyses reveal that Futsch loops are more abundant during earlier stages of synapse assembly than at maturity (compare larvae at 108 hours AEL with wandering third instars). In *dfmr1*-nulls, Futsch loops are significantly more abundant, both during active synapse growth and at maturity. These results suggest that the dynamic growth capacity of the synapse is reflected by the number of Futsch loops as a function of developmental time and, thus, that *dfmr1* mutants are arrested in a premature growth state.

Presynaptic induction of dFMRP totally fails to rescue the elevated cycling of synaptic vesicles in the *dfmr1*-null mutant, indicating that this defect has its origin in a postsynaptic function of dFMRP. The known postsynaptic function at the *Drosophila* NMJ is selection of the appropriate glutamate receptor classes, with relative abundances dramatically skewed by the absence of dFMRP (Pan and Broadie, 2007). Therefore, our results suggest that defects in the postsynaptic glutamate receptor field cause a compensatory change in the presynaptic vesicle cycling underlying glutamate release, presumably via a trans-synaptic retrograde signal (Davis et al., 1998; Frank et al., 2006; Paradis et al., 2001; Petersen et al., 1997). In support of this hypothesis, a recent study showed that presynaptic *Fmr1* genotype influences synaptic connectivity in a mosaic mouse model, with neurons lacking FMRP being less likely to form functional synapses (Hanson and Madison, 2007). Conversely, acute postsynaptic expression of FMRP in *Fmr1* KO neurons results in a decrease in the number of functional and structural synapses relative to neighboring untransfected neurons, indicating phenotypic rescue (Pfeiffer and Huber, 2007). Although it is possible that pre- and postsynaptic effects are independent of one another, trans-synaptic compensation warrants consideration in dissecting the spatial requirement of FMRP in modulating synaptic function.

Temporal requirements for FMRP: development versus plasticity

In mice, the appearance of *Fmr1* mutant phenotypes is age-dependent, with at least some defects appearing transiently. In layer V barrel cortex, KO neurons display abnormal dendritic spine length/density during cortical synaptogenesis early in development (postnatal week 1); however, these differences are undetectable by week 4 (Galvez and Greenough, 2005; Nimchinsky et al., 2001). Functionally, mutant mice display brain-region-specific defects in both LTD and LTP (Huber et al., 2002; Larson et al., 2005; Li et al., 2002; Nosyreva and Huber, 2006; Wilson and Cox, 2007). However, it is important to realize that such defects may reflect either an acute FMRP function in the adult animal or, just as easily, a transient role of FMRP during development that pre-establishes the ability of synapses to manifest plasticity at maturity. Indeed, synaptic plasticity defects appear to be much more severe during transient developmental windows, with less severe defects at maturity (Huang et al., 2006).

The GS system allows rapid induction of *dfmr1* transcription, but an inherent limitation to the approach rests with the protein half-life. We show here that the dFMRP protein appears relatively stable, with a half-life of ~26 hours. Thus, we can switch ‘on’ dFMRP within a few hours, but the switch ‘off’ is governed by the protein decay profile over the course of several days, limiting temporal resolution. For this reason, we restricted analyses to two intervention windows. First, we employed a 12-hour induction immediately after hatching, carefully determining the induction strength to ensure a match with endogenous dFMRP protein levels. With this treatment, dFMRP levels decrease exponentially with time; the protein was almost undetectable by ~60 hours post-treatment. Second, a brief 12-hour induction at the terminal endpoint of larval life was executed. Again, we carefully controlled induction specific to this mature time point, to match levels of the introduced protein to dFMRP levels in the control. With this protocol, the animals completely lacked all dFMRP throughout development, with acute protein reintroduction immediately prior to analysis at maturity.

In the early induction paradigm, transient dFMRP expression yields almost complete rescue of *dfmr1*-null synaptic structural defects, including expansion of the synaptic terminal area, overbranching of synaptic processes, and the formation of excess synaptic boutons. The resolution towards wild-type architecture indicates a primarily early role for dFMRP in molding the NMJ, and suggests that dFMRP-mediated imprinting/patterning of synaptic development allows for appropriate and sustainable synaptic structure. These findings support the conclusion that dFMRP is required early for proper initiation of synaptogenesis and not synaptic maintenance. This conclusion is perhaps not unexpected for a protein that acts as a translational regulator of synaptogenic proteins, which will have their own perdurance at the synapse once properly regulated by early dFMRP function. In addition, however, acute dFMRP induction at maturity provides partial rescue of

synaptic architecture defects. This effect is a true rescue, i.e. resolution of overgrowth phenotypes that are fully manifest at the start of the transgene expression window. This finding demonstrates that the established NMJ synapse displays morphological plasticity and can be remodeled. These findings are in agreement with presynaptically mediated remodeling in which synapse retraction occurs, trailing a postsynaptic 'footprint' (Eaton et al., 2002; Pielage et al., 2005). Such regression would be requisite in mediating the observed rescue of *dfmr1*-null overgrowth via bouton destabilization and elimination.

Much work continues to be focused on alleviating FraX symptoms and targeting the causative molecular insults resulting in the disease state. Recent work in the *Fmr1* KO mouse has shown rescue, at cellular and behavioral levels, via constitutive reduction in mGluR5 (Dolen et al., 2007) and p21-activated kinase (Hayashi et al., 2007). Translation of these exciting new findings into clinical treatments will be better informed with the temporal requirement of FMRP clearly defined. In future work, we will test the efficacy of targeted temporal interventions in both mGluR-mediated signaling upstream of FMRP function, as well as translational consequences downstream of FMRP function.

We are especially grateful to Dr Haig Keshishian (Yale University) for the *elav*-Gene-Switch line that made this work possible. We thankfully acknowledge the Bloomington *Drosophila* Stock Center and the Iowa Developmental Studies Hybridoma Bank for genetic lines and antibodies, respectively. We thank Dr Elisabeth Dykens (Vanderbilt Kennedy Center for Research on Human Development) for her role in providing clinical co-mentorship to C.L.G. during this project; members of the Broadie laboratory, especially Dr Charles Tessier, for insightful discussion; Drs Sarah Repicky, Jeffrey Rohrbough and Kevin Haas, and Ms. Ashleigh Long for technical training, suggestions and support with regard to the electrophysiology studies presented. This work was funded by the National Institutes of Health through the NIH Roadmap for Medical Research Training Grant T32 MH075883 to C.L.G. and R01 grant GM54544 to K.B.

References

Antar, L. N., Afroz, R., Dictenberg, J. B., Carroll, R. C. and Bassell, G. J. (2004). Metabotropic glutamate receptor activation regulates fragile X mental retardation protein and FMR1 mRNA localization differentially in dendrites and at synapses. *J. Neurosci.* **24**, 2648-2655.

Ashley, J., Packard, M., Ataman, B. and Budnik, V. (2005). Fasciclin II signals new synapse formation through amyloid precursor protein and the scaffolding protein dX11/Mint. *J. Neurosci.* **25**, 5943-5955.

Bailey, D. B., Jr, Hatton, D. D., Skinner, M. and Mesibov, G. (2001a). Autistic behavior, FMR1 protein, and developmental trajectories in young males with fragile X syndrome. *J. Autism Dev. Disord.* **31**, 165-174.

Bailey, D. B., Jr, Hatton, D. D., Tassone, F., Skinner, M. and Taylor, A. K. (2001b). Variability in FMRP and early development in males with fragile X syndrome. *Am. J. Ment. Retard.* **106**, 16-27.

Bear, M. F., Huber, K. M. and Warren, S. T. (2004). The mGluR theory of fragile X mental retardation. *Trends Neurosci.* **27**, 370-377.

Bettencourt da Cruz, A., Schwarzel, M., Schulze, S., Niyyati, M., Heisenberg, M. and Kretzschmar, D. (2005). Disruption of the MAP1B-related protein FUTSCH leads to changes in the neuronal cytoskeleton, axonal transport defects, and progressive neurodegeneration in Drosophila. *Mol. Biol. Cell* **16**, 2433-2442.

Beumer, K. J., Rohrbough, J., Prokop, A. and Broadie, K. (1999). A role for PS integrins in morphological growth and synaptic function at the postembryonic neuromuscular junction of Drosophila. *Development* **126**, 5833-5846.

Brumback, A. C., Lieber, J. L., Angleson, J. K. and Betz, W. J. (2004). Using FM1-43 to study neuropeptide granule dynamics and exocytosis. *Methods* **33**, 287-294.

Castets, M., Schaeffer, C., Bechara, E., Schenck, A., Khandjian, E. W., Luche, S., Moine, H., Rabilloud, T., Mandel, J. L. and Bardoni, B. (2005). FMRP interferes with the Rac1 pathway and controls actin cytoskeleton dynamics in murine fibroblasts. *Hum. Mol. Genet.* **14**, 835-844.

Comery, T. A., Harris, J. B., Willems, P. J., Oostra, B. A., Irwin, S. A., Weiler, I. J. and Greenough, W. T. (1997). Abnormal dendritic spines in fragile X knockout mice: maturation and pruning deficits. *Proc. Natl. Acad. Sci. USA* **94**, 5401-5404.

Cornish, K. M., Munir, F. and Cross, G. (2001). Differential impact of the FMR-1 full mutation on memory and attention functioning: a neuropsychological perspective. *J. Cogn. Neurosci.* **13**, 144-150.

Davis, G. W., DiAntonio, A., Petersen, S. A. and Goodman, C. S. (1998). Postsynaptic PKA controls quantal size and reveals a retrograde signal that regulates presynaptic transmitter release in Drosophila. *Neuron* **20**, 305-315.

Dent, E. W. and Kalil, K. (2001). Axon branching requires interactions between dynamic microtubules and actin filaments. *J. Neurosci.* **21**, 9757-9769.

Dickman, D. K., Lu, Z., Meinertzhagen, I. A. and Schwarz, T. L. (2006). Altered synaptic development and active zone spacing in endocytosis mutants. *Curr. Biol.* **16**, 591-598.

Dockendorff, T. C., Su, H. S., McBride, S. M., Yang, Z., Choi, C. H., Siwicki, K. K., Sehgal, A. and Jongens, T. A. (2002). Drosophila lacking dfmr1 activity show defects in circadian output and fail to maintain courtship interest. *Neuron* **34**, 973-984.

Dolen, G., Osterweil, E., Rao, B. S., Smith, G. B., Auerbach, B. D., Chattarji, S. and Bear, M. F. (2007). Correction of fragile X syndrome in mice. *Neuron* **56**, 955-962.

Eaton, B. A., Fetter, R. D. and Davis, G. W. (2002). Dynactin is necessary for synapse stabilization. *Neuron* **34**, 729-741.

Einfeld, S., Hall, W. and Levy, F. (1991). Hyperactivity and the fragile X syndrome. *J. Abnorm. Child Psychol.* **19**, 253-262.

Fergestad, T. and Broadie, K. (2001). Interaction of stoned and synaptotagmin in synaptic vesicle endocytosis. *J. Neurosci.* **21**, 1218-1227.

Ferrari, F., Mercaldo, V., Piccoli, G., Sala, C., Cannata, S., Achsel, T. and Bagni, C. (2007). The fragile X mental retardation protein-RNP granules show an mGluR-dependent localization in the post-synaptic spines. *Mol. Cell. Neurosci.* **34**, 343-354.

Frank, C. A., Kennedy, M. J., Goold, C. P., Marek, K. W. and Davis, G. W. (2006). Mechanisms underlying the rapid induction and sustained expression of synaptic homeostasis. *Neuron* **52**, 663-677.

Galvez, R. and Greenough, W. T. (2005). Sequence of abnormal dendritic spine development in primary somatosensory cortex of a mouse model of the fragile X mental retardation syndrome. *Am. J. Med. Genet. A* **135**, 155-160.

Gould, E. L., Loesch, D. Z., Martin, M. J., Hagerman, R. J., Armstrong, S. M. and Huggins, R. M. (2000). Melatonin profiles and sleep characteristics in boys with fragile X syndrome: a preliminary study. *Am. J. Med. Genet.* **95**, 307-315.

Hanson, J. E. and Madison, D. V. (2007). Presynaptic FMR1 genotype influences the degree of synaptic connectivity in a mosaic mouse model of fragile X syndrome. *J. Neurosci.* **27**, 4014-4018.

Hayashi, M. L., Rao, B. S., Seo, J. S., Choi, H. S., Dolan, B. M., Choi, S. Y., Chattarji, S. and Tonegawa, S. (2007). Inhibition of p21-activated kinase rescues symptoms of fragile X syndrome in mice. *Proc. Natl. Acad. Sci. USA* **104**, 11489-11494.

Hinton, V. J., Brown, W. T., Wisniewski, K. and Rudelli, R. D. (1991). Analysis of neocortex in three males with the fragile X syndrome. *Am. J. Med. Genet.* **41**, 289-294.

Huang, Z., Shimazu, K., Woo, N. H., Zang, K., Muller, U., Lu, B. and Reichardt, L. F. (2006). Distinct roles of the beta 1-class integrins at the developing and the mature hippocampal excitatory synapse. *J. Neurosci.* **26**, 11208-11219.

Huber, K. M., Gallagher, S. M., Warren, S. T. and Bear, M. F. (2002). Altered synaptic plasticity in a mouse model of fragile X mental retardation. *Proc. Natl. Acad. Sci. USA* **99**, 7746-7750.

Hummel, T., Krukkert, K., Roos, J., Davis, G. and Klambt, C. (2000). Drosophila Futsch/22C10 is a MAP1B-like protein required for dendritic and axonal development. *Neuron* **26**, 357-370.

Inoue, S., Shimoda, M., Nishinokubi, I., Siomi, M. C., Okamura, M., Nakamura, A., Kobayashi, S., Ishida, N. and Siomi, H. (2002). A role for the Drosophila fragile X-related gene in circadian output. *Curr. Biol.* **12**, 1331-1335.

Irwin, S. A., Patel, B., Idupulapati, M., Harris, J. B., Crisostomo, R. A., Larsen, B. P., Kooy, F., Willems, P. J., Cras, P., Kozlowski, P. B. et al. (2001). Abnormal dendritic spine characteristics in the temporal and visual cortices of patients with fragile-X syndrome: a quantitative examination. *Am. J. Med. Genet.* **98**, 161-167.

Jan, L. Y. and Jan, Y. N. (1976). Properties of the larval neuromuscular junction in Drosophila melanogaster. *J. Physiol. (Lond)* **262**, 189-214.

Koukoui, S. D. and Chaudhuri, A. (2007). Neuroanatomical, molecular genetic, and behavioral correlates of fragile X syndrome. *Brain Res. Rev.* **53**, 27-38.

Larson, J., Jessen, R. E., Kim, D., Fine, A. K. and du Hoffmann, J. (2005). Age-dependent and selective impairment of long-term potentiation in the anterior piriform cortex of mice lacking the fragile X mental retardation protein. *J. Neurosci.* **25**, 9460-9469.

Li, J., Pelletier, M. R., Perez Velazquez, J. L. and Carlen, P. L. (2002). Reduced cortical synaptic plasticity and GluR1 expression associated with fragile X mental retardation protein deficiency. *Mol. Cell. Neurosci.* **19**, 138-151.

Lu, R., Wang, H., Liang, Z., Ku, L., O'Donnell, W. T., Li, W., Warren, S. T. and Feng, Y. (2004). The fragile X protein controls microtubule-associated protein 1B translation and microtubule stability in brain neuron development. *Proc. Natl. Acad. Sci. USA* **101**, 15201-15206.

McGuire, S. E., Roman, G. and Davis, R. L. (2004). Gene expression systems in Drosophila: a synthesis of time and space. *Trends Genet.* **20**, 384-391.

Michel, C. I., Kraft, R. and Restifo, L. L. (2004). Defective neuronal development in the mushroom bodies of Drosophila fragile X mental retardation 1 mutants. *J. Neurosci.* **24**, 5798-5809.

Morales, J., Hiesinger, P. R., Schroeder, A. J., Kume, K., Verstreken, P., Jackson, F. R., Nelson, D. L. and Hassan, B. A. (2002). Drosophila fragile X protein, DFXR, regulates neuronal morphology and function in the brain. *Neuron* **34**, 961-972.

Muddashetty, R. S., Kelic, S., Gross, C., Xu, M. and Bassell, G. J. (2007). Dysregulated metabotropic glutamate receptor-dependent translation of AMPA receptor and postsynaptic density-95 mRNAs at synapses in a mouse model of fragile X syndrome. *J. Neurosci.* **27**, 5338-5348.

Munir, F., Cornish, K. M. and Wilding, J. (2000). Nature of the working memory deficit in fragile-X syndrome. *Brain Cogn.* **44**, 387-401.

Nimchinsky, E. A., Oberlander, A. M. and Svoboda, K. (2001). Abnormal development of dendritic spines in FMR1 knock-out mice. *J. Neurosci.* **21**, 5139-5146.

Nosyreva, E. D. and Huber, K. M. (2006). Metabotropic receptor-dependent long-term depression persists in the absence of protein synthesis in the mouse model of Fragile X Syndrome. *J. Neurophysiol.* **95**, 3291-3295.

Osterwalder, T., Yoon, K. S., White, B. H. and Keshishian, H. (2001). A conditional tissue-specific transgene expression system using inducible GAL4. *Proc. Natl. Acad. Sci. USA* **98**, 12596-12601.

Pan, L. and Broadie, K. S. (2007). Drosophila fragile X mental retardation protein and metabotropic glutamate receptor A convergently regulate the synaptic ratio of ionotropic glutamate receptor subclasses. *J. Neurosci.* **27**, 12378-12389.

Pan, L., Zhang, Y. Q., Woodruff, E. and Broadie, K. (2004). The Drosophila fragile X gene negatively regulates neuronal elaboration and synaptic differentiation. *Curr. Biol.* **14**, 1863-1870.

Pan, L., Woodruff, E., 3rd, Liang, P. and Broadie, K. (2008). Mechanistic relationships between Drosophila fragile X mental retardation protein and metabotropic glutamate receptor A signaling. *Mol. Cell. Neurosci.* **37**, 747-760.

Paradis, S., Sweeney, S. T. and Davis, G. W. (2001). Homeostatic control of presynaptic release is triggered by postsynaptic membrane depolarization. *Neuron* **30**, 737-749.

Penagarikano, O., Mulle, J. G. and Warren, S. T. (2007). The pathophysiology of fragile X syndrome. *Annu. Rev. Genomics Hum. Genet.* **8**, 109-129.

Petersen, S. A., Fetter, R. D., Noordermeer, J. N., Goodman, C. S. and DiAntonio, A. (1997). Genetic analysis of glutamate receptors in Drosophila reveals a retrograde signal regulating presynaptic transmitter release. *Neuron* **19**, 1237-1248.

Pfeiffer, B. E. and Huber, K. M. (2007). Fragile X mental retardation protein induces synapse loss through acute postsynaptic translational regulation. *J. Neurosci.* **27**, 3120-3130.

Pielage, J., Fetter, R. D. and Davis, G. W. (2005). Presynaptic spectrin is essential for synapse stabilization. *Curr. Biol.* **15**, 918-928.

Plomp, J. J., van Kempen, G. T. and Molenaar, P. C. (1992). Adaptation of quantal content to decreased postsynaptic sensitivity at single endplates in alpha-bungarotoxin-treated rats. *J. Physiol.* **458**, 487-499.

Reeve, S. P., Bassetto, L., Genova, G. K., Kleyner, Y., Leyssen, M., Jackson, F. R. and Hassan, B. A. (2005). The Drosophila fragile X mental retardation protein controls actin dynamics by directly regulating profilin in the brain. *Curr. Biol.* **15**, 1156-1163.

Rohrbough, J., Rushton, E., Palanker, L., Woodruff, E., Matthies, H. J., Acharya, U., Acharya, J. K. and Broadie, K. (2004). Ceramidase regulates synaptic vesicle exocytosis and trafficking. *J. Neurosci.* **24**, 7789-7803.

Roos, J., Hummel, T., Ng, N., Klambt, C. and Davis, G. W. (2000). Drosophila Futsch regulates synaptic microtubule organization and is necessary for synaptic growth. *Neuron* **26**, 371-382.

Rudelli, R. D., Brown, W. T., Wisniewski, K., Jenkins, E. C., Laure-Kamionowska, M., Connell, F. and Wisniewski, H. M. (1985). Adult fragile X syndrome. Clinico-neuropathologic findings. *Acta Neuropathol.* **67**, 289-295.

Ruiz-Canada, C., Ashley, J., Moeckel-Cole, S., Drier, E., Yin, J. and Budnik, V. (2004). New synaptic bouton formation is disrupted by misregulation of microtubule stability in aPKC mutants. *Neuron* **42**, 567-580.

Sabaratnam, M., Vroegop, P. G. and Gangadharan, S. K. (2001). Epilepsy and EEG findings in 18 males with fragile X syndrome. *Seizure* **10**, 60-63.

Sandrock, A. W., Jr, Dryer, S. E., Rosen, K. M., Gozani, S. N., Kramer, R., Theill, L. E. and Fischbach, G. D. (1997). Maintenance of acetylcholine receptor number by neuregulins at the neuromuscular junction in vivo. *Science* **276**, 599-603.

Tanaka, E. M. and Kirschner, M. W. (1991). Microtubule behavior in the growth cones of living neurons during axon elongation. *J. Cell Biol.* **115**, 345-363.

Todd, P. K., Mack, K. J. and Malter, J. S. (2003). The fragile X mental retardation protein is required for type-I metabotropic glutamate receptor-dependent translation of PSD-95. *Proc. Natl. Acad. Sci. USA* **100**, 14374-14378.

Torroja, L., Packard, M., Gorczyca, M., White, K. and Budnik, V. (1999). The Drosophila beta-amyloid precursor protein homolog promotes synapse differentiation at the neuromuscular junction. *J. Neurosci.* **19**, 7793-7803.

Tsui, H. T., Lankford, K. L., Ris, H. and Klein, W. L. (1984). Novel organization of microtubules in cultured central nervous system neurons: formation of hairpin loops at ends of maturing neurites. *J. Neurosci.* **4**, 3002-3013.

Wilson, B. M. and Cox, C. L. (2007). Absence of metabotropic glutamate receptor-mediated plasticity in the neocortex of fragile X mice. *Proc. Natl. Acad. Sci. USA* **104**, 2454-2459.

Zalfa, F., Eleuteri, B., Dickson, K. S., Mercaldo, V., De Rubeis, S., di Penta, A., Tabolacci, E., Chiurazzi, P., Neri, G., Grant, S. G. et al. (2007). A new function for the fragile X mental retardation protein in regulation of PSD-95 mRNA stability. *Nat. Neurosci.* **10**, 578-587.

Zhang, Y. Q., Bailey, A. M., Matthies, H. J., Renden, R. B., Smith, M. A., Speese, S. D., Rubin, G. M. and Broadie, K. (2001). Drosophila fragile X-related gene regulates the MAP1B homolog Futsch to control synaptic structure and function. *Cell* **107**, 591-603.